Photoreverse Reaction Dynamics of Octopus Rhodopsin

Keiichi Inoue,* Motoyuki Tsuda,† and Masahide Terazima*
*Graduate School of Science, Kyoto University, Sakyo-ku, Kyoto, Japan; and †Graduate School of Life Science, University of Hyogo, Chuo-ku, Kobe, Japan

ABSTRACT Photoreverse reactions of octopus rhodopsin (Rh) from acid-metarhodopsin (Acid-Meta), which is the final product of the photoreaction of Rh, to Rh were studied by the time-resolved transient absorption and transient grating methods. The time course of the absorption signal showed a rapid change within 500 ns followed by one phase with a time constant of ~470 μs, whereas the transient grating signal indicates three phases with time constants of <500 ns, ~490 μs, and 2.6 ms. The faster two phases indicate the conformational change in the vicinity of the chromophore, and the slowest one represents conformational change far from the chromophore. The absorption spectrum of the first intermediate created just after the laser excitation (<500 ns) is already very similar to the final product, Rh. This behavior is quite different from that of the forward reaction from Rh to Acid-Meta, in which several intermediates with different absorption spectra are involved within 50 ns–500 μs. This result indicates that the conformation around the chromophore is easily adjusted from all-*trans* to 11-*cis* forms compared with that from 11-*cis* to all-*trans* forms. Furthermore, it was found that the protein energy is quickly relaxed after the excitation. One of the significantly different properties between Rh and Acid-Meta is the diffusion coefficient (*D*). *D* is reduced by about half the transformation from Rh to Acid-Meta. This large reduction was interpreted in terms of the helix opening of the Rh structure.

INTRODUCTION

Rhodopsins (Rhs) are photoreceptors discovered in rod outer segments in the retina of various animals. The Rhs absorb visible light and, through several intermediate states, are activated to transfer a signal to the following guanine nucleotide-binding proteins (G-protein). Eventually, they generate electric signals for visual sensing of the light (1,2). The Rhs are a prototype of G-protein coupled-reactor family proteins, which consist of seven transmembrane helices. Because the Rhs can be activated by light, they have been presented as one of the best systems for revealing the reaction dynamics in a time domain.

The reaction dynamics and the intermediates of the Rhs have been studied extensively (3,4). After photoexcitation of the retinal chromophore, the 11-*cis* to all-*trans* isomerization reaction takes place within picoseconds (5). Although the triggering reaction is ultrafast, the protein part does not respond as quickly, and the following thermal reactions proceed in a range of nanoseconds to seconds with several intermediates. This dynamics should represent how the protein responds to the conformational change of the retinal chromophore. Such a protein response to the external stimuli should be essential for understanding many biological responses. On this point, it would be interesting to consider how fast the protein responds for a reverse change of the chromophore (from all-*trans* to 11-*cis*) compared with the forward reaction (from 11-*cis* to all-*trans*). If the protein conformation is optimized for the 11-*cis* form of retinal chromophores, the reverse reaction could be very fast. On the other hand, if the reaction proceeds backward along a similar reaction pathway to that of the forward reaction and the energetic barriers are similar, the reaction dynamics might be similar to the forward one. Unfortunately, such a reverse reaction is difficult to examine for vertebrate Rhs (except the photoregeneration experiments on bovine Rh from one of the intermediates (6)) (vide infra) because vertebrate Rhs are dissociated into the apoprotein and retinal chromophore eventually after the forward reaction. In this respect, invertebrate Rhs have unique features such that they keep the chromophore in its binding pocket even after conversion to the final product. In particular, octopus Rh (7), which is one of the prototypes of invertebrate Rhs, is converted to the final product, the acid-metarhodopsin (Acid-Meta) state, by blue light illumination and this Acid-Meta is returned to the original Rh state by irradiation of orange light. Therefore, this octopus Rh gives us a valuable opportunity to study the reverse process of the chromophore.

Whereas the forward photoreaction dynamics of octopus Rh has been studied by several spectroscopic methods (8–13), the reverse photoreaction process from Acid-Meta to Rh has not been studied in detail. In this work, we studied this photoreverse reaction dynamics by two different spectroscopic methods to observe the changes in different parts of the protein. We used the traditional flash photolysis method to monitor the conformational changes in the vicinity of the chromophore part. We also used a pulsed laser-induced transient grating (TG) method to study the global conformational change of octopus Rh in addition to the chromophore part. Since the TG signal can detect the partial molar volume change during chemical reaction, we expect that any reaction step including a spectrally silent one can be monitored.

We furthermore studied the conformational difference between Rh and Acid-Meta from the viewpoint of the

Submitted November 27, 2006, and accepted for publication January 29, 2007.

Address reprint requests to Masahide Terazima, Tel.: 81-75-753-4026; Fax: 81-75-753-4026; E-mail: mterazima@kuchem.kyoto-u.ac.jp.

0006-3495/07/05/3643/09 $2.00

doi: 10.1529/biophysj.106.101741

translational diffusion coefficient (D). Although there are several physical properties to characterize the protein conformation, D is a unique property, which reflects the intermolecular interaction between the protein and solvent molecules including the protein conformation or surface roughness. For example, the unfolding of the secondary structure was detected during a protein-folding reaction (14) or a photoreaction (15) in time domain. Interestingly, we found that D of Acid-Meta is much smaller than that of Rh. This difference is interpreted in terms of the increase of protein-water interaction by dislocating the helices. We consider this D-change to be a common feature of the photoreaction of photosensor proteins.

MATERIAL AND METHODS

Laser light from an Nd:YAG laser ($\lambda = 532$ nm, Quantum-Ray model GCR-170-10, Spectra-Physics, Mountain View, CA) was used to pump a dye laser ($\lambda = 560$ nm with Rhodamine 6G dye, GSTR-LG-24-us, Sirah Laser- und Plasmatechnik, Kaarst, Germany), and this dye laser light was used for the excitation of a sample solution. For recording the absorption change in a range from near-ultraviolet to a visible region at various delay times after the excitation, light from a Xe-lamp (probe light) was introduced to the sample under counterpropagation geometry against the excitation light. The probe light passing through the sample was led to a monochrometer by an optical fiber and detected by an intensified charge-coupled device camera system (PI-MAX/PI-MAX2 System, Roper Scientific, Trenton, NJ). The intensity at each wavelength was integrated during a certain time period and recorded by a computer. For measuring the time development of the absorption change at a specific wavelength, the light from the Xe-lamp passed through a blue band-pass filter ($\lambda_{max} = 420$ nm, full width at half-maximum = 10 nm, Edmund Optics Japan, Tokyo, Japan) was used for the probe light. The change of the probe light intensity was monitored by a photomultiplier and accumulated by a digital oscilloscope (Tektronix TDS-520, Beaverton, OR). To avoid the effect of the accumulated photoproduct in the illuminated region, the sample solution was stirred and irradiated by blue light (light from a tungsten lamp or overhead projector with a cutoff filter ($\lambda < \sim 450$ nm)) after every irradiation of the pulsed excitation light.

The experimental setup for the TG measurement was similar to that reported previously (12,16–18). Briefly, the excitation laser beam was split into two by a beam splitter and crossed inside a sample cell. A continuous wave laser light from a diode laser ($\lambda = 840$ nm) was used for the probe light. A part of the probe beam diffracted by the refractive index modulation was detected by a photomultiplier tube, and the temporal profile was recorded by a digital oscilloscope. Usually, 100 signals at each condition were averaged to improve the signal/noise ratio. To remove the accumulated photoproduct from the light-illuminated region, the sample solution was stirred and irradiated by the blue light in the same way transient absorption measurements are. For a measurement in a fast timescale, the TG signals were recorded with a repetition rate of 0.23 Hz under continuous stirring.

For transient absorption and TG measurements, the absorbance of the sample in a buffer with 0.04% β-D-fructopyranosyl-α-D-glucopyranoside (SM1200, Dojindo, Kumaoto, Japan), 10 mM Tris-HCl (pH = 7.4) was adjusted to 0.5 (protein concentration = 80 μM) in a 2-mm optical path length quartz cell. The sample solution was filtered by a cellulose acetate membrane filter (Cosmospin Filter G (pore size = 0.2 μm); Nacalai tesque Kyoto, Japan) to remove dust contained in the quartz cell. Any scattering probe light from the sample solution was carefully removed to avoid any heterodyne contribution to the TG signal. Moreover, we solubilized the sample protein in different detergents (cyclohexyl-butyl-β-D-maltoside (CYMAL-4), cyclohexyl-pentyl-β-D-maltoside (CYMAL-5), and cyclohexyl-hexyl-β-D-maltoside (CYMAL-6) (Anatrace, Maumee, Ohio) to study the effect on the hydrophobic tail length of detergent molecules.

For far-ultraviolet ($\lambda = 190$–250 nm) circular dichroism (CD) measurements, the concentration of Rh was adjusted to 2.5 μM. The sample solution was contained in the quartz cell and measured by a spectrometer (J720W1, JASCO, Tokyo, Japan) with flowing N_2 gas.

For the sample protein, truncated octopus Rh (19) was used to study in a homogenous system (no isoforms). Microvillar membranes of octopus photoreceptors were prepared from eyes of *Octopus defleini* as described previously (20), and octopus Rh was purified from the membrane by the method of Tsuda et al. (21). The procedure of purification of Rh was described by Ashida et al. (19). Octopus microvillar membranes (containing 5 mg/ml Rh) were incubated with 1 mg/ml *Staphylococcus aureus* V-8 protease (Wako, Osaka, Japan) with a Rh/enzyme ratio of 280:1 (mol/mol) in 50 mM Tris-HCl buffer, pH 7.4, at 15°C for 1 h. Under these conditions, ~½ of the Rh was not digested, but with longer incubation times cleavage of the 5-6 intracellular loop of Rh started (22,23). After the digestion, the membranes were suspended with a buffer containing 0.5% 3-[(3-cholamidopropyl)dimethylammonio]propane-1-sulfonic acid (CHAPS) (Wako), 50 mM Tris-HCl, pH 7.4, and 1 mM dithiothreitol (DTT), and peripheral proteins were removed by centrifugation at 200,000 × g for 30 min.

Washed membranes were solubilized with 1.2% (w/v) nonyl-glucoside (NG, Anatrace) in 50 mM Tris-HCl, pH 7.4, and 1 mM DTT and diluted threefold with 50 mM Tris-HCl, pH 7.4, and centrifuged at 200,000 × g for 30 min to remove the insoluble fraction. The mixture was fractionated with 61% ammonium sulfate (Sigma, St. Louis, MO). The supernatant was dialyzed against a solution containing 0.01% dodecyl-maltoside (DDM, Anatrace), 10 mM Tris-HCl, pH 7.4, and 1 mM DTT and applied to a monolithic diethylaminoethyl (DEAE) column (1.5 cm × 4.5 cm, BIA, Ljubljana, Slovenia) which had been equilibrated with 10 mM Tris-HCl, pH 7.4, 1 mM DTT, and 0.05% DDM. The column was thoroughly washed with the equilibrate buffer until absorbance at 280 nm returned to the baseline; then the proteins were eluted with NaCl. The fractions were assayed by absorption spectroscopy and sodium dodecylsulfate-polyacrylamide gel electrophoresis. Rh was eluted at ~40 mM NaCl as a single peak.

PRINCIPLE

The optical grating is created by the interference of the two excitation-pulsed laser beams. There are several origins for the TGs. One of the dominant contributions is the temperature change of the medium induced by the energy from the nonradiative decay of excited states and by the enthalpy change (ΔH) of the reaction (thermal grating $\delta n_{th}(t)$). Another important contribution originates from change in the absorbance of the solution: the population grating. The partial molecular volume (V) difference between the reactant and products (ΔV) induces a change in the average density of the medium, and this change causes the refractive index change: volume grating. A term of 'the species grating' is used to describe both of these contributions. If the contribution of absorbance change at the probe wavelength is negligible and the diffraction efficiency of the probe light is small, the TG signal intensity is proportional to the square of the peak-null difference of the refractive index created by the interference pattern of the excitation light intensity (12,16,24).

$$I_{TG}(t) = \alpha\{\delta n_{th}(t) + \delta n_{spe}(t)\}^2, \quad (1)$$

where α is a constant.

The temporal profile of the refractive index grating due to the thermal grating is given by

$$\delta n_{\mathrm{th}}(t) = \{(dn/dT)/\rho C_{\mathrm{P}}\}\{(dQ(t)/\mathrm{d}t) * \exp(-D_{\mathrm{th}}q^2 t)\}, \quad (2)$$

where * is the convolution integral, $Q(t)$ is the thermal energy coming out from the sample, dn/dT is the temperature dependence of the refractive index, ρ is the density, C_{p} is the heat capacity at a constant pressure, and D_{th} is the thermal diffusivity. By comparing the thermal grating intensity with that of a calorimetric reference sample, which releases all excitation energy as heat within our experimental time response, under the same condition, the enthalpy change of a reaction can be determined (13,18,24,25).

The refractive index change due to the volume change (δn_{v}) is given by (13,18,24,25)

$$\delta n_{\mathrm{v}} = V\frac{dn}{dV}\,\Delta V \Delta N,$$

where Vdn/dV is the refractive index change by the molecular volume change. By taking a ratio of $\delta n_{\mathrm{v}}/\delta n_{\mathrm{th}}$ of a calorimetric reference sample with the known solvent property (Vdn/dV), ΔV was determined from the signal intensity (13,18,24,25).

The time dependence of the species grating is determined by the kinetics of the reaction and the molecular diffusion process. If we can ignore the reaction kinetics, the time dependence is given by (12,16,24)

$$\delta n_{\mathrm{spe}}(t) = -\delta n_{\mathrm{r}} \exp(-D_{\mathrm{r}}q^2 t) + \delta n_{\mathrm{p}} \exp(-D_{\mathrm{p}}q^2 t), \quad (3)$$

where q is a grating wavenumber and δn_{r} and δn_{p} represent refractive index changes by the reactant and product, respectively. D_{r} and D_{p} are the diffusion coefficients of the reactant and product, respectively. The reaction kinetics can be separated from the diffusion process by measuring the TG signal at different q^2, because the signal decay rate due to the diffusion depends on q^2, whereas the reaction kinetics should not.

RESULTS AND DISCUSSION

Transient absorption

Fig. 1 *a* depicts the absorption spectra of Rh. Upon continuous blue light (420 nm) illumination to the sample solution, the absorption spectrum changes to a red-shifted one, which represents the photoconversion from Rh to Acid-Meta. Photochemical reaction intermediates during this reaction have been studied by monitoring the absorption change (11,12). It has been reported that the absorption spectrum changes by three phases with time constants of 110 ns, 360 ns, and 23 μs within a time range of 100 ns–1 s. This kinetics has been explained by the decay time constants of bathorhodopsin (Batho), lumirhodopsin (Lumi), and mesorhodopsin (Meso), respectively.

The absorption spectrum of the final product Acid-Meta is depicted in Fig. 1 *a*, which was constructed from the absorption spectrum under the continuous blue light illumination by subtracting the spectrum of Rh with a reported fraction of Rh (30%) under this condition (26). The spectrum of Acid-Meta is red-shifted ~21 nm compared with that of Rh.

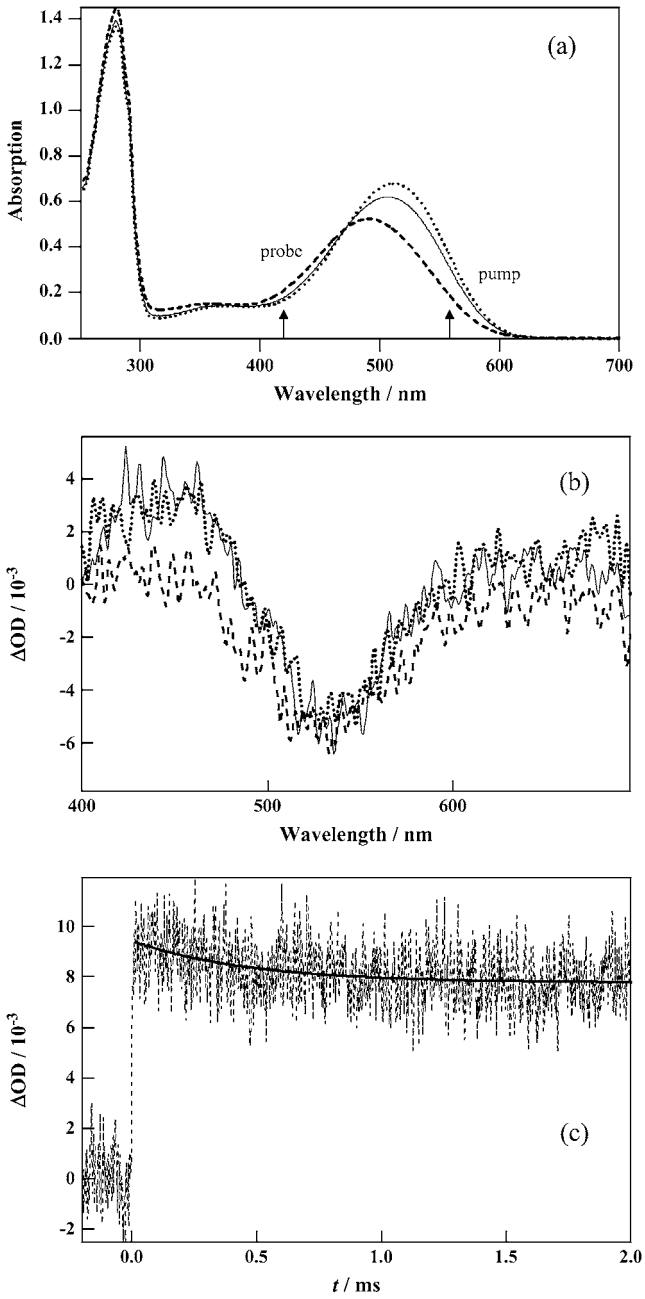

FIGURE 1 (*a*) Absorption spectra of Rh in the dark (*broken line*) and under the continuous blue light ($\lambda \approx 420$ nm) irradiation (*solid line*) conditions. The absorption spectrum of Acid-Meta (*dotted line*) was calculated by subtracting the contribution of 30% Rh from the blue light irradiated spectrum. The pump and probe wavelengths for the transient absorption measurements are indicated by arrows. (*b*) Transient difference absorption spectra of reverse photoreaction of Rh monitored at 27 μs (*solid line*), 107 μs (*dotted line*), and 16 ms (*broken line*). (*c*) Time development of the transient absorption change in a few milliseconds time region (*broken line*). The pump and probe wavelength were 560 and 420 nm, respectively. The best-fitted curve by the single exponential function with a constant term is shown by the solid line.

For studying the photoreaction of Acid-Meta (reverse reaction), we first illuminated the sample solution by the blue light to accumulate Acid-Meta and excited this solution by orange light $\lambda = 560$ nm. Since the fraction of Acid-Meta

under the blue light illumination is 70% (19) and the molar absorption coefficients of Acid-Meta is six times higher than Rh at this wavelength (19), a large fraction of the orange light (93%) was used for the excitation of Acid-Meta. Even though the quantum yields of the forward reaction (0.69) is slightly larger than that of the reverse reaction (0.43) (27), the dominant photoreaction under this condition is the reverse reaction. Fig. 1 *b* shows the pump light induced absorption spectra change at some delay times after the excitation. The bleached spectrum peaked at 535 nm represents the depletion of Acid-Meta. The enhanced absorption was observed in a range of 420–490 nm. The intensity of this absorption decreased with increasing delay time.

The temporal profile of the absorption change was monitored at a single wavelength (center wavelength = 420 nm, full width at half-maximum = 10 nm) and is depicted in Fig. 1 *c*. The absorption at this wavelength increased within a time response of our system (500 ns), decreased with a lifetime of 470 ± 60 μs, and did not change further within our observation time range (<100 ms). Since no time constant of the forward reaction kinetics (11,12) was observed, a possible (minor) contribution from the Rh reaction in this signal can be ignored. From this profile, it is apparent that Acid-Meta is not converted to Rh directly, but at least one short-lived (470 μs) intermediate species (I_1) exists. This intermediate is transferred to a long-lived species, which exists at least within 100 ms after the excitation.

The absorption spectra of this I_1 intermediate and long-lived species were constructed from the difference spectra in short (10–35 μs) and long (4.3–21 ms) time regions by subtracting the original (Acid-Meta) spectrum (Fig. 2). Both of the absorption spectra are very similar to that of Rh (λ_{max} = 491 nm). The similar spectrum of I_1 to that of Rh suggests that the all-*trans* retinal chromophores in Acid-Meta are converted to 11-*cis* retinal chromophores very quickly and the protein conformation close to the chromophore is already similar to that of Rh within 500 ns. In particular, the spectrum of the long-lived species is almost identical to that of Rh, suggesting that this long-lived species is the final product: Rh. However, since we cannot completely exclude the possibility of spectral silent dynamics, the TG signal was measured as described in the next section.

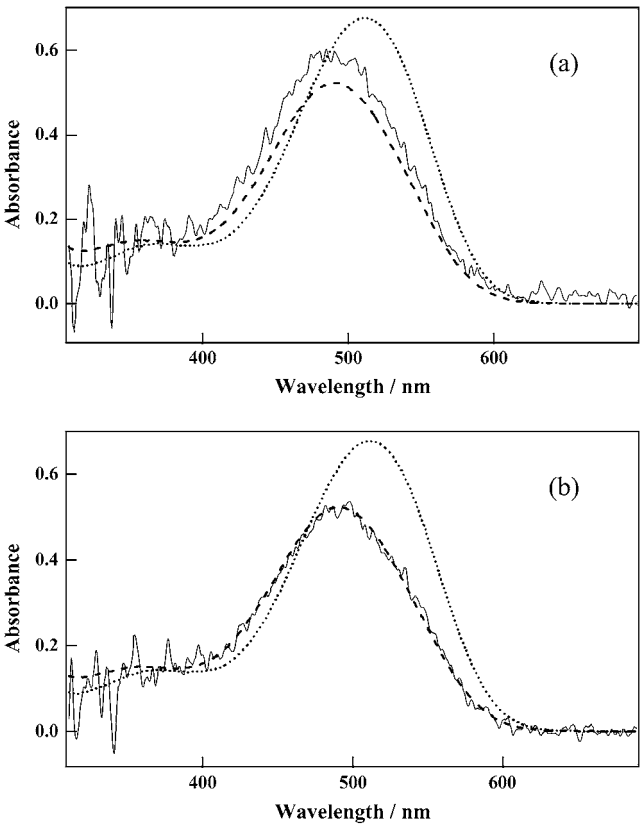

FIGURE 2 Calculated absorption spectra of (*a*) the first and (*b*) the second intermediate species observed in transient absorption measurement (*solid lines*). The broken and dotted lines represent the absorption spectra of Rh and Acid-Meta calculated by the method described in the text.

Reaction dynamics monitored by transient grating

The transient absorption and its kinetics have been generally used to identify and characterize the reaction intermediate species in chemistry and biochemistry. However, the absorption spectrum change reflects only changes of the chromophore and its vicinity. To study the conformational changes in the whole protein, we used the TG technique. For comparison purpose, before describing the TG signal of the reverse reaction, we first briefly show the TG signal of the forward reaction of Rh. Fig. 3 depicts the TG signal after photoexcitation of Rh at 465 nm with $q^2 = 6.1 \times 10^{11}$ m^{-2}. The features of the TG signal were already described in an earlier work (12). Briefly, the signal rose within 10 ns after the photoexcitation followed by several decaying components and rising components. The signal in a whole time range (100 ns–400 ms) was well expressed by a sum of seven exponential functions. Among them, three of the rate constants depended on the grating wavenumber (q^2) and the other did not.

The q^2-dependent components represent the diffusion processes, and the q^2-indepenent components are due to chemical reactions, not the diffusion. The time constant of the fastest q^2-dependent component (decay component in 10^{-5}-s range in Fig. 3) was the same as that of the thermal grating signal after the photoexcitation of the calorimetric reference aqueous solution (Bromocresol purple), so that this component should be attributed to the thermal grating signal, and the time constant is given by $1/\tau_{th} = D_{th}q^2$ (Eq. 2). The other q^2-dependent kinetics (the latest peak in Fig. 3) represents the protein diffusion processes. The diffusing species was assigned based on the signs of the refractive index changes. From a curve fitting of the signal and the fact that the refractive index change of the thermal grating is negative at this temperature ($\delta n_{th} < 0$), we determined the signs of the refractive index changes for the rise and decay components of

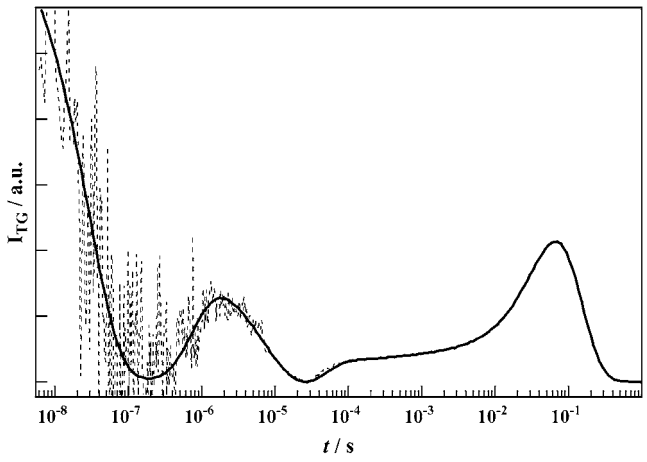

FIGURE 3 TG signal of forward photoreaction of Rh measured at $q^2 = 6.1 \times 10^{11}\ m^{-2}$ (*broken line*). The best-fitted line by Eq. 4 is shown by the solid line. The fitted line is almost completely overlapped by the observed signal.

the diffusion peak signal to be negative and positive, respectively (12). Comparing with Eq. 3, we identified the chemical species for the rise and decay signals to Rh and Acid-Meta, respectively. Hence, the time profile of the TG signal over this wide time range (10 ns ~ 400 ms) can be expressed by

$$I_{TG}(t) = \alpha\{\delta n_A \exp(-t/\tau_A) + \delta n_B \exp(-t/\tau_B) + \delta n_{th} \exp(-t/\tau_{th}) + n_C \exp(-t/\tau_C) + \delta n_D \exp(-t/\tau_D) - \delta n_E \exp(-D_{Rh} q^2 t) + \delta n_F \exp(-D_{Acid} q^2 t)\}^2, \quad (4)$$

where δn_i ($i = A$–F and th) are preexponential factors of these exponential terms, $\tau_A < \tau_B < \tau_C < \tau_D$. Furthermore, D_{Rh} and D_{Acid} are the diffusion coefficients of Rh and Acid-Meta, respectively, ($D_{Rh} > D_{Acid}$). By the curve fitting of the signal, τ_A, τ_B, τ_C, and τ_D were determined to be 64 ns, 480 ns, 25 μs, and 490 μs. On the basis of the reported assignment using the absorption change, τ_A, τ_B, and τ_C correspond to the decay time constants of Batho, Lumi, and Meso, respectively. The slowest kinetics, 490 μs, does not appear in the absorption change. This spectrally silent process indicates that there is another intermediate, transient Acid-Meta (Tr-Acid-Meta). Hence the forward reaction scheme of Rh is Rh → Batho → Lumi → Meso → Tr-Acid-Meta → Acid-Meta.

We measured the TG signal of the preilluminated sample by the blue light for measuring the reverse reaction dynamics at $q^2 = 6.1 \times 10^{11}\ m^{-2}$. This observed signal mainly comes from the photoreaction of Acid-Meta (reverse reaction), but the minor contribution of the forward photoreaction of Rh should be subtracted from this signal. This contribution was estimated by the same method described in the previous section. We estimated that the signal of Acid-Meta should be 8.7 times stronger than Rh at this condition. The TG signal of the forward reaction reduced by this ratio was subtracted from the observed TG signal. Both TG signals of the forward and reverse reaction were normalized by the amplitudes of the diffusion signal (i.e., δn_E and δn_F of Eq. 4 and δn_3 and δn_4 of Eq. 5). Fig. 4 shows the TG signal of the reverse reaction calculated this way.

The features of the TG signal of the reverse reaction are quite different from that of the forward reaction. This signal was expressed by the sum of five exponentials (*solid line* in Fig. 4). For the assignment of these components, we measured the signals under various grating wavenumbers and found that three time constants depended on the q^2-value, whereas two of them were independent. Since one of the time constants was the same as that of the thermal grating signal of the calorimetric reference sample, this component should be attributed to the thermal grating signal. Similar to the forward reaction, the latest peak is due to the protein diffusion. Hence, the TG signal can be expressed by

$$I_{TG}(t) = \alpha\{\delta n_{th} \exp(-t/\tau_{th}) + \delta n_1 \exp(-t/\tau_1) - \delta n_2 \exp(-t/\tau_2) + \delta n_3 \exp(-D_3 q^2 t) - \delta n_4 \exp(-D_4 q^2 t)\}^2, \quad (5)$$

where $\tau_1 < \tau_2$. From the curve fitting, the signs of the amplitudes of these terms were determined as δn_1 and δn_3 are positive and δn_2 and δn_4 are negative. First we describe the intrinsic reaction, and the analysis of diffusion will be presented in the next section.

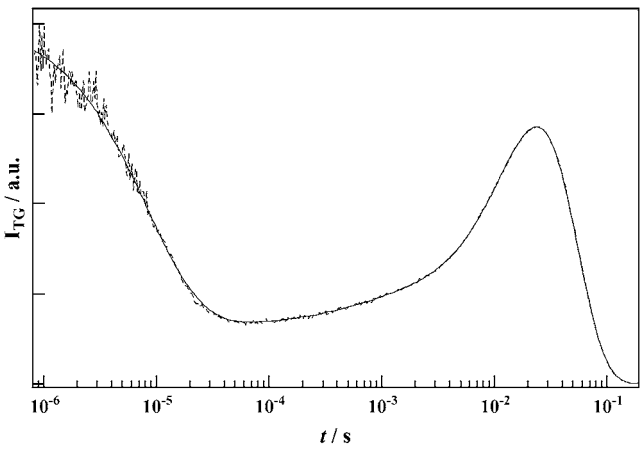

FIGURE 4 TG signal of reverse photoreaction of Rh at $q^2 = 6.1 \times 10^{11}\ m^{-2}$ (*broken line*). The best-fitted curve by Eq. 5 is shown by the solid line. The fitted line is almost completely overlapped with the observed signal.

The lifetimes of the second and the third terms of Eq. 5 were independent of the q^2-value, and these were determined to be 490 ± 140 μs and 2.6 ± 1.4 ms, respectively. Since the decay time of I_1 (470 μs) described in the previous section is close enough to that of the first component within the experimental uncertainty, we consider that τ_1 represents the decay of I_1.

The slower kinetics with the time constant of 2.6 ms was observed only by the TG method. Hence, this is a spectrally silent process, which reflects conformational change apart from the chromophore. As described in the Principle section, the origin of the species grating comes from the population grating (absorption change) and/or the volume grating. Since there is no absorption change, we attributed this TG component to the volume grating. The negative sign of this component indicates the volume contraction on this step. From the amplitude of the refractive index change, the volume change was calculated to be -2.9 ± 1.0 ml mol^{-1} by the method described in the Principle section. Previously, Nishioku et al. reported that the partial molar volume increases from Rh to Acid-Meta on the forward reaction (13). The volume contraction observed in this study is considered to be the volume recovery process during the reverse reaction; that is, a part of the increased protein volume of Acid-Meta is relaxed in this millisecond time region. The reaction scheme determined in this study is depicted in Fig. 5.

In the case of vertebrate Rh, the Schiff base of the physiologically activated state (Meta II) is deprotonated. In contrast to octopus Rh, the illumination of blue light to Meta II does not recover the dark-adapted state, but it yields the Meta III state, which is generally produced thermally from Meta II in parallel with dissociation of retinal and opsin parts (6,28). However, it was found that the intermediates preceding Meta II, in which the Schiff bases are protonated, are converted to the dark-adapted state by absorbing a second photon (6). These results may suggest that the protonated Schiff base enables the intermediate to be recovered to the dark-adapted state upon photoexcitation, and the recovery is inhibited by the deprotonation. Therefore, for octopus Rh, the protonated Shiff base of Acid-Meta could be important to provide the photoreversal function. The molecular mechanism of the photorecovery process should be clarified by further studies on both vertebrate and invertebrate Rhs.

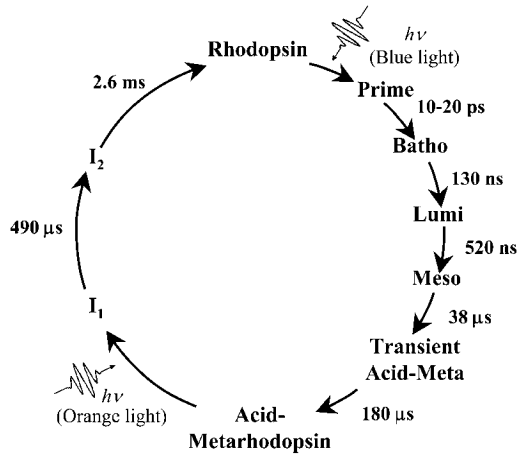

FIGURE 5 Schematic diagrams of photoreaction dynamics of Rh for forward and reverse reactions.

Comparing with the thermal grating signal intensity from the calorimetric reference sample, we noted that the intensity of the thermal grating signal of the reverse reaction is much stronger than that of the forward reaction. Since the thermal grating intensity represents the released energy from the photoexcited protein, the stronger thermal grating intensity means that most of the photon energy is released. From the thermal grating intensity of the Acid-Meta sample and the calorimetric reference sample under the same experimental condition, we determined ΔH of the first intermediate I_1 to be 9 ± 10 kJ mol^{-1}.

Previously, ΔH of all intermediates in the forward reaction was determined (13). According to the results, ΔH of Rh, to Batho, Lumi, Meso, Tr-Acid-Meta, and Acid-Meta were 146 kJ mol^{-1}, 122 kJ mol^{-1}, 38 kJ mol^{-1}, 12 kJ mol^{-1}, and 12 kJ mol^{-1} from the initial state, respectively. Since the energy of the lowest excited state of bovine Rh is 222 kJ mol^{-1} (29), it was found that most of the energy (65%) is stored in the first (Batho) intermediate. On the other hand, in the case of the reverse reaction, most of the absorbed photon energy is released, i.e., the first intermediate that is formed within 500 ns is already energetically stabilized. This enthalpy is similar to those of Tr-Acid-Meta and Acid-Meta on the forward reaction. Therefore, we concluded that the dominant part of the protein conformation is relaxed in a fast time range.

In the case of vertebrate Rh, later photoproducts have relatively higher enthalpy, e.g., $\Delta H = 70.3$ kJ mol^{-1} and 115 kJ mol^{-1} for the metarhodopsin I and metarhodopsin II states, respectively (30). The large ΔH of vertebrate Rh intermediates are considered to be necessary for the photodissociation and releasing of all-*trans* retinal chromophores from the opsin. For octopus Rh, because the activated protein does not need to break the linkage between retinal and opsin, the energy is used only for the faster dynamics of protein relaxation and slow dynamics seems to be entropy driven.

Diffusion change

The latest peak of the TG signal represents the protein diffusion process. D of Rh and Acid-Meta were determined from the q^2 dependence of the rate constants of the rise and decay components, respectively. From the TG signal of the forward reaction (Fig. 3), D_{Rh} and D_{Acid} were determined to be $6.0 \pm 0.2 \times 10^{-11}$ m^{2}s^{-1} and $2.8 \pm 0.3 \times 10^{-11}$ m^{2}s^{-1}, respectively. For the reverse reaction (Fig. 4), they were $D_{Rh} = 6.13 \pm 0.08 \times 10^{-11}$ m^{2}s^{-1} and $D_{Acid} = 2.91 \pm 0.09 \times 10^{-11}$ m^{2}s^{-1}. The determined D of both species from the forward and reverse reactions agrees well within the experimental error. This fact confirms that the forward and reverse

reactions complete within the time range of the TG measurement; i.e., there is no slower conformational change.

When does this D-change take place? If D changes during the protein diffusion time, the D-value becomes time dependent. The equation that describes the time-dependent D was reported previously (14,15,31,32). This equation is similar to Eq. 5, but the rate constant of the exponential term of Eq. 5 is given by not only D but also the rate constant (k) of the D-change: $\exp(-(k + Dq^2)t)$. Therefore, from the q^2 dependence of the TG signal, we can determine D and the rate of the D-change. We found that the observed TG signals measured at various q^2 (data not shown) could be fitted well by Eq. 5, which does not contain an additional rate constant. This fact indicates a rather rapid D-change, i.e., it completes before the appearance of the diffusion signal, at least faster than 3 ms. There is a possibility that the rate of D-change is the same as that of the volume changes (2.6 ms).

One of the most striking features of the observed TG signal is that D_{Rh} and D_{Acid} are significantly different. What is the molecular origin of this change? According to the Stokes-Einstein equation, D of a spherical molecule is expressed by

$$D = \frac{k_B T}{a\eta r}, \tag{6}$$

where k_B, T, η, a, and r are Boltzmann constant, temperature, viscosity, a constant representing the boundary condition between the diffusing molecule and the solvent, and the radius of the molecule, respectively. First we examined the possibility of a protein volume expansion to be the cause of the large (~½) reduction in D for Acid-Meta.

To account for the reduction of D by one-half, the molecular volume of Acid-Meta should expand almost eight times compared to Rh. Naturally, it is unrealistic to consider such a large volume expansion of the protein alone. Alternatively, this volume expansion could be due to the increase in the size of the protein-micellar complex by the aggregation of additional detergent molecules around Acid-Meta. If this is the case, we estimated that ~1300 additional detergent molecules are accumulated around the Acid-Meta species (the molecular volume of the detergent molecule is ~430 ml mol^{-1} (0.72 nm^3/molecule, (33)). For bacteriorhodopsin, the number of detergent molecules surrounding one protein molecule was reported to be ~100 molecules (33). Since the architectures in the transmembrane region between Rh and bacteriorhodopsin are similar, it may be reasonable to assume that Rh is also surrounded by a similar number of detergents in the ground state. Therefore, to account for the reduction of D, more than 10 times more detergent molecules should be accumulated around Acid-Meta. We believe that accumulation of such a large number of detergent molecules is physically impossible. Furthermore, it is possible to gather such a large number of detergent molecules in neither milliseconds nor a faster timescale. To examine if the detergent molecules are involved in the reduction process of D, we measured the TG signal in various detergent solutions, such as CYMAL-4, -5, -6. The diffusion coefficients of Rh and Acid-Meta solubilized in these surfactants are listed in Table 1. Although CYMAL-5 has a somewhat smaller D_{Rh} and larger D_{Acid} compared to those in other types of detergent, we did not find any systematic dependence of D on the hydrophobic tail length of the detergent molecule. This suggests that change in D should not be caused by change of protein-detergent complex size.

It is well known that not only molecular size but also intermolecular interaction governs the D-value. For example, it was reported that Ds of various proteins decrease when their secondary structures (α-helix) are unfolded (14,34). This reduction in D was explained by the increase of the intermolecular interaction between the protein and water molecules, which is induced by the exposure of amino acid residues to bulk water. A similar phenomenon was observed in a photoreaction of light oxygen volotage domains (15). Since Rh consists of α-helices in its structure, one may expect D-reduction by the unfolding of the α-helices to increase the protein-solvent interaction. This unfolding mechanism was examined by measuring the α-helix contents in both Rh and Acid-Meta from the CD spectra (Fig. 6). The shape of the CD spectrum of Rh in the $\lambda > 210$ nm region was similar to that of bovine Rh (35). The negative peak at $\lambda = 220$ nm indicates that Rh consists of α-helices. It is important to note that the CD spectrum measured under the blue light irradiation was very similar to that of Rh and Acid-Meta. This fact indicates that the α-helix content is not changed by the photoconversion. Hence we concluded that α-helix unfolding is not the main reason for the decrease in D of Rh.

In the case of bovine Rh, the opening of the cytoplasmic side (separation of the cytoplasmic ends of TM III and TM VI) and the increase of solvent accessibility to the inside of the helix bundle has been suggested by previous studies (36,37). We may suggest that a similar movement of the α-helices occurs by the photoreaction of Rh. If the interaction of amino acid residues and water molecules strengthened in this newly exposed area, the friction of the protein molecule could be increased. A significant D-change by the changes in the intermolecular interaction has been established by a number of articles (14,15,17,31,34). Another possible explanation for the enhanced intermolecular interaction could be related to the conformational change in the C-terminal extension. Octopus Rh has an extensively long sequence in the C-terminal and is considered to exist in the outside of plasma membrane (7). Even in the case of the truncated form, ~40 residues remain as

TABLE 1 Diffusion coefficients of Rh and Acid-Meta solubilized in various surfactants

Surfactants	$D_{Rh}/10^{-11}$ m^2/s	$D_{Acid\text{-}Meta}/10^{-11}$ m^2/s
SM-1200	6.13 ± 0.08	2.91 ± 0.09
CYMAL-4	6.26 ± 0.10	4.48 ± 0.07
CYMAL-5	6.39 ± 0.10	4.3 ± 0.05
CYMAL-6	6.06 ± 0.03	3.70 ± 0.2

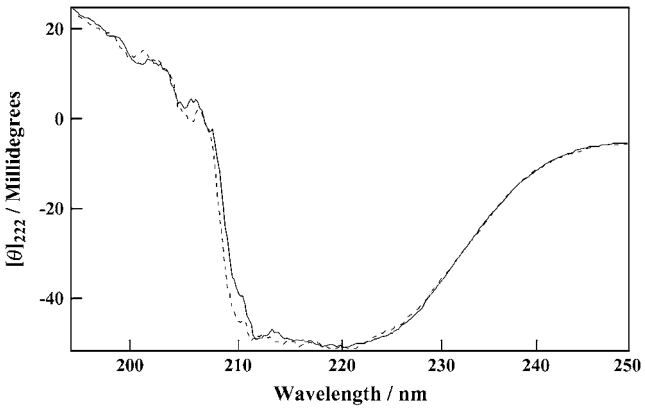

FIGURE 6 CD spectra of Rh in the dark (*solid line*) and illuminated by blue light (*broken line*).

C-terminal extension. If the conformation of this region is changed so that the intermolecular interaction with water increases, D of Acid-Meta should be smaller than Rh. At present, we do not know which part of the protein is responsible for the reduction of D. This point should be examined in future using mutants of Rh.

An important observation in this study is the diffusion-sensitive conformational change, which reflects the intermolecular interaction, occurs, and we consider that such movement may be related to the physiological function, activation of the G-protein. Indeed, similar diffusion-sensitive conformational changes were observed in signaling states of various photosensor proteins, such as LOV2 proteins (15,31), AppA (32), photoactive yellow protein (38,39), and phytochrome (40). We may speculate from these data, including the result of Rh, that the diffusion-sensitive conformational change is a common feature of photosensor proteins for the signal transduction.

SUMMARY

To study the reverse photoreaction dynamics and the conformational change of octopus Rh, the transient absorption and TG techniques were used in time domain. The transient absorption spectrum and the time profile of the absorption signal showed that the conformation in the vicinity of the chromophore changes within 500 ns and a time constant of 470 μs. The transient absorption spectrum showed that the conformation around the chromophore has almost completely adjusted to the 11-*cis* form within 500 ns. This behavior is quite different from that of the forward reaction from Rh to Acid-Meta, in which several intermediates with different absorption spectra are involved. The time profile of the TG signal showed that the reverse reaction takes place in time constants of $<$500 ns, 490 μs, and 2.6 ms. The slowest dynamics was interpreted in terms of the molecular volume change due to the conformational change far from the chromophore. It was found that the energy of the protein is quickly relaxed after the isomerization. Furthermore, it was surprising to find that the diffusion coefficient of Acid-Meta was drastically reduced from that of Rh. This large reduction was interpreted in terms of the α-helix relocation to lead to the opening of the cytoplasmic side or the conformational change in the C-terminal extension. At present, we speculate that the diffusion-sensitive conformational changes could be a common feature of photosensor proteins for the signal transduction.

This work was supported by a grant-in-aid (Nos. 13853002 and 15076204) from the Ministry of Education, Science, Sports and Culture in Japan.

REFERENCES

1. Ridge, K. D., N. G. Abdulaev, M. Sousa, and K. Palczewski. 2003. Phototransduction:crystal clear. *Trends Biochem. Sci.* 28:479–487.
2. Briggs, W. R., and J. L. Spudich, editors. 2005. Handbook of Photosensory Receptors. Wiley, Weinheim, Germany.
3. Hug, S. J., J. L. Lewis, C. M. Einterz, T. E. Thorgeirsson, and D. S. Kliger. 1990. Nanosecond photolysis of rhodopsin: evidence for a new, blue-shifted intermediate. *Biochemistry.* 29:1475–1485.
4. Kliger, D. S., and J. W. Lewis. 1995. Spectral and kinetic characterization of visual pigment photointermediates. *Isr. J. Chem.* 35:289–307.
5. Schoenlein, R. W., L. A. Peteanu, R. A. Mathies, and C. V. Shank. 1991. The first step in vision: femtosecond isomerization of rhodopsin. *Science.* 254:412–415.
6. Ritter, E., K. Zimmermann, M. Heck, K. P. Hofmann, and F. J. Bartl. 2004. Transition of rhodopsin into the active metarhodopsin II state opens a new light-induced pathway linked to Schiff base isomerization. *J. Biol. Chem.* 279:48102–48111.
7. Ovchinnikov, Y. A., N. G. Abdulaev, A. S. Zolotarev, I. D. Artamonov, I. A. Bespalov, A. E. Dergachev, and M. Tsuda. 1988. Octopus rhodopsin amino acid sequence deduced from cDNA. *FEBS Lett.* 232:69–72.
8. Ohtani, H., T. Kobayashi, M. Tsuda, and T. G. Ebrey. 1988. Primary processes in photolysis of octopus rhodopsin. *Biophys. J.* 53:17–24.
9. Deng, H., D. Manor, G. Weng, P. Rath, Y. Koutalos, T. Ebrey, R. Gebhard, J. Lugtenburg, M. Tsuda, and R. H. Callender. 1991. Resonance Raman studies of the HOOP modes in octopus bathorhodopsin with deuterium-labeled retinal chromophores. *Biochemistry.* 30:4495–4502.
10. Taiji, M., K. Bryl, M. Nakagawa, M. Tsuda, and T. Kobayashi. 1992. Femtosecond studies of primary photoprocesses in octopus rhodopsin. *Photochem. Photobiol.* 56:1003–1011.
11. Nakagawa, M., S. Kikkawa, T. Iwasa, and M. Tsuda. 1997. Light-induced protein conformational changes in the photolysis of octopus rhodopsin. *Biophys. J.* 72:2320–2328.
12. Nishioku, Y., M. Nakagawa, M. Tsuda, and M. Terazima. 2001. A spectrally silent transformation in the photolysis of octopus rhodopsin: a protein conformational change without any accompanying change of chromophore's absorption. *Biophys. J.* 80:2922–2927.
13. Nishioku, Y., M. Nakagawa, M. Tsuda, and M. Terazima. 2002. Energetics and volume changes of intermediates in the photolysis of octopus rhodopsin at physiological temperature. *Biophys. J.* 83:1136–1146.
14. Nishida, S., T. Nada, and M. Terazima. 2004. Kinetics of intermolecular interaction during protein folding of reduced cytochrome *c*. *Biophys. J.* 87:2663–2675.
15. Eitoku, T., Y. Nakasone, D. Matsuoka, S. Tokutomi, and M. Terazima. 2005. Conformational dynamics of phototropin 2 LOV2 domain with the linker upon photoexcitation. *J. Am. Chem. Soc.* 127:13238–13243.

16. Terazima, M., and N. Hirota. 1993. Translational diffusion of a transient radical studied by the transient grating method, pyrazinyl radical in 2-propanol. *J. Chem. Phys.* 98:6257–6262.

17. Terazima, M. 2000. Is the translational diffusion of organic radicals different from that of closed-shell molecules? *Acc. Chem. Res.* 33: 687–694.

18. Sakakura, M., I. Morishima, and M. Terazima. 2001. The structural dynamics and ligand releasing process after the photodissociation of sperm whale carboxymyoglobin. *J. Phys. Chem.* 105:10424–10434.

19. Ashida, A., K. Matsumoto, T. G. Ebrey, and M. Tsuda. 2004. A purified agonist-activated G-protein coupled receptor: truncated octopus acid metarhodopsin. *Zoolog. Sci.* 21:245–250.

20. Tsuda, M., H. Hirata, and T. Tsuda. 1992. Interaction of rhodopsin, G-protein and kinase in octopus photoreceptors. *Photochem. Photobiol.* 56:1167–1172.

21. Tsuda, M., T. Tsuda, Y. Terayama, Y. Fukada, T. Akino, G. Yamanaka, L. Stryer, T. Katada, M. Ui, and T. G. Ebrey. 1986. Kinship of cephalopod photoreceptor G-protein with vertebrate transducin. *FEBS Lett.* 198:5–10.

22. Tsuda, M. 1979. Optical activity of octopus metarhodopsin. *Biochim. Biophys. Acta.* 578:372–380.

23. Tsuda, M. 1988. Signal coupling proteins in octopus photoreceptors. *In* Molecular Physiology of Retinal Proteins. T. Hara, editor. Yamada Science Foundation, Osaka, Japan. 167–172.

24. Hara, T., N. Hirota, and M. Terazima. 1996. New application of the transient grating method to a photochemical reaction: the enthalpy, reaction volume change, and partial molar volume measurements. *J. Phys. Chem.* 100:10194–10200.

25. Inoue, K., J. Sasaki, M. Morisaki, F. Tokunaga, and M. Terazima. 2004. Time-resolved detection of sensory rhodopsin II-transducer interaction. *Biophys. J.* 87:2587–2597.

26. Kitagawa, T., and M. Tsuda. 1980. Resonance Raman-spectra of octopus acid and alkaline metarhodopsins. *Biochim. Biophys. Acta.* 624: 211–217.

27. Dixon, S. F., and A. Cooper. 1987. Quantum efficiencies of reversible photoreaction of octopus rhodopsin. *Photochem. Photobiol.* 46:115–119.

28. Bartl, F. J., E. Ritter, and K. P. Hofmann. 2001. Signaling states of rhodopsin. *J. Biol. Chem.* 276:30161–30166.

29. Guzzo, A. V., and G. L. Pool. 1968. Visual pigment fluorescence. *Science.* 159:312–314.

30. Cooper, A. 1981. Rhodopsin photoenergetics: lumirhodopsin and the complete energy profile. *FEBS Lett.* 123:324–326.

31. Nakasone, Y., T. Eitoku, D. Matsuoka, S. Tokutomi, and M. Terazima. 2006. Kinetic measurement of transient dimerization and dissociation reactions of *Arabidopsis* phototropin 1 LOV2 domain. *Biophys. J.* 91: 645–653.

32. Hazra, P., K. Inoue, W. Laan, K. J. Hellingwerf, and M. Terazima. 2006. Tetramer formation kinetics in the signaling state of AppA monitored by time-resolved diffusion. *Biophys. J.* 91:654–661.

33. Møller, J. V., and M. Maire. 1993. Detergent binding as a measure of hydrophobic surface area of integral membrane proteins. *J. Biol. Chem.* 268:18659–18672.

34. Inoue, K., N. Baden, and M. Terazima. 2005. Diffusion coefficient and the secondary structure of poly-L-glutamic acid in aqueous solution. *J. Phys. Chem. B.* 109:22623–22628.

35. Liu, X., P. Garriga, and H. G. Khorana. 1996. Structure and function in rhodopsin: correct folding and misfolding in two point mutants in the intradiscal domain of rhodopsin identified in retinitis pigmentosa. *Proc. Natl. Acad. Sci. USA.* 93:4554–4559.

36. Farrens, D. L., C. Altenbach, K. Yang, W. L. Hubbell, and H. G. Khorana. 1996. Requirement of rigid-body motion of transmembrane helices for light activation of rhodopsin. *Nature.* 274:768–770.

37. Abdulaev, N. G., and K. D. Ridge. 1998. Light-induced exposure of the cytoplasmic end of transmembrane helix seven in rhodopsin. *Proc. Natl. Acad. Sci. USA.* 95:12854–12859.

38. Takeshita, K., Y. Imamoto, M. Kataoka, F. Tokunaga, and M. Terazima. 2002. Thermodynamic and transport properties of intermediate states of the photocyclic reaction of photoactive yellow protein. *Biochemistry.* 41:3037–3048.

39. Khan, J. S., Y. Imamoto, M. Harigai, M. Kataoka, and M. Terazima. 2006. Conformational changes of PYP monitored by diffusion coefficient: effect of N-terminal α-helices. *Biophys. J.* 90:3686–3693.

40. Eitoku, T., X. Zarate, G. V. Kozhukh, J. -I. Kim, P.-S. Song, and M. Terazima. Time-resolved detection of conformational changes in oat phytochrome A: time-dependent diffusion. *Biophys. J.* 91:3797–3804.